HAIL DETECTION DURING THE JOINT POLARIZATION EXPERIMENT

Pamela L. Heinselman and Alexander V. Ryzhkov

Cooperative Institute for Mesoscale Meteorological Studies
University of Oklahoma
Norman, OK 73019

1. Introduction

In the spring of 2003, polarimetric data were collected at the National Severe Storms Laboratory (NSSL) in support of the Joint Polarization Experiment (JPOLE). JPOLE was motivated by the potential for polarimetric applications to improve rainfall estimation, segregation of meteorological and nonmeteorological echo, and hydrometeor classification. The goals of JPOLE were to evaluate the engineering design and data quality of a polarimetric prototype of the Weather Surveillance Radar-1988 Doppler (WSR-88D) radar (KOUN), demonstrate the utility of the data in applications, and collect data for cost-benefit analysis and future research.

Recent studies of JPOLE datasets validate significant improvements in rainfall estimation (Ryzhkov et al. 2003) and hydrometeor classification by the National Severe Storm Laboratory's hydrometeor classification algorithm (HCA; Schuur et al. 2003), compared to conventional WSR-88D algorithms. One important component of the HCA, hail detection, is the focus of this paper.

Corresponding author address: Pamela Heinselman, CIMMS/Univ. of Oklahoma, 1313 Halley Circle, Norman, OK, 73069.
E-mail: Pam.Heinselman@noaa.gov

Conventional approaches to hail detection have distinct disadvantages compared to polarimetric approaches. These disadvantages are discussed with respect to the current WSR-88D hail detection algorithm (HDA; Witt et al. 1998). First, HDA is based on vertical storm structure and environmental conditions that are difficult to quantify. Second, relationships between these factors and the probability of hail (severe or nonsevere) are empirically derived, rather than based on hydrometeor properties. Third, hail probabilities characterize the storm as a whole, so that the hail location is not specified.

Unlike conventional radar variables, polarimetric variables are directly related to hydrometeor properties useful for pinpointing the location of hail within a storm. Previous research indicates that polarimetric variables such as differential reflectivity (Z_{DR}; Aydin et al. 1986), linear depolarization ratio (LDR; Hubbert et al. 1998; Kennedy et al. 2001), correlation coefficient (ρ_{HV}; Balakrishnan and Zrnic 1990; hereafter BZ 1990), and specific differential phase (K_{DP}; BZ 1990) are instrumental for hail detection. These variables are defined in detail in Bringi and Chandrasekar (2001). While earlier approaches to hail detection apply $Z-Z_{DR}$ relations to separate rain from hail (Aydin et al. 1986), more recent approaches employ fuzzy logic. In the fuzzy logic approach, membership

functions determine the degree to which various polarimetric measurements represent the likelihood of hail (Vivekananan et al. 1999; Zrnić and Ryzhkov 1999; Straka et al. 2000; Liu and Chandrasekar 2000, and Zrnić et al. 2001). To date, validation of these approaches is limited to case studies, without systematic statistical assessment of several hail events.

The purpose of this paper is to assess and compare the performance of the recently tuned HCA to both its earlier version and the conventional HDA. This assessment employs a ground truth dataset of 74 rain and hail reports, from 8 storms, collected by hail intercept crews during JPOLE. The HCA and HDA are described in section 2, followed by an overview of data collection during JPOLE and the employed verification methodology in section 3. Section 4 describes the results, and section 5 provides a summary and conclusions.

2. Algorithm descriptions

Both the JPOLE (JPHCA) and more recent version of HCA are based on principles of fuzzy logic, as outlined in Vivekanandan et al. (1999), Zrnić and Ryzhkov (1999), Straka et al. (2000), Liu and Chadrasekar (2000), and Zrnić et al. (2001). Following JPOLE, studies of JPHCA resulted in two significant changes to the algorithm. First, the fuzzy logic methodology was transformed by using one-dimensional membership functions in place of two-dimensional membership functions (e.g., Schuur et al. 2003). Consequently, only membership functions based on Z_{DR} depend on a second variable—reflectivity factor, Z.
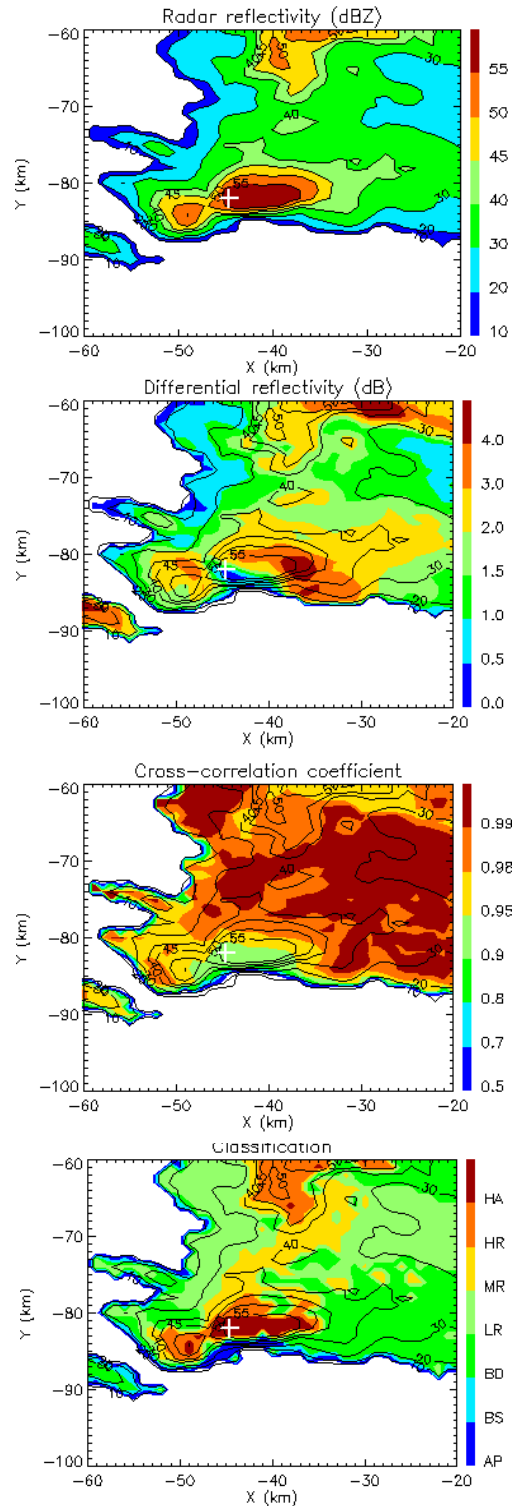

Figure 1. Fields of (a) radar reflectivity, (b) differential reflectivity, (c) JPHCA output, and (d) cross-correlation coefficient at 23:10 UTC on 11 June 2003. The plus sign indicates the location of 2.5 cm hail detected by the hail intercept team.

Second, the more recent version of HCA employs six, rather than three, variables for classification. While both versions identify hail by high values of Z combined with low Z_{DR} and ρ_{hv} (Aydin et al. 1986; Balakrishnan and Zrnić 1990; Smith et al. 1999; among others), the new version also uses texture parameters to characterize the depth of spatial oscillations of Z and Φ_{DP} (SD(Z) and SD(Φ_{DP}), respectively), and Doppler velocity V, to distinguish between hail and ground clutter/AP, which might have a very similar Z, Z_{DR}, and ρ_{hv}. Low V and high values of the texture variables characterize ground clutter. This automated methodology is used to detect seven different classes including ground clutter / anomalous propagation (GC/AP), biological scatterers (BS), big drops (BD), light rain (LR), moderate rain (MR), heavy rain (HR), and rain/hail mixture (HA) at the two lowest scans (0.5˚ and 1.5˚).

Figure 1 shows a representative example of JPHCA output for a supercell storm whose core is located approximately 40 km west and 80 km south of KOUN at 23:10 UTC on 11 June 2003. In Fig. 1, the reported hail (white plus sign) is located in a region where reflectivity (55 dBZ or higher), Z_{DR} (0.0–0.5), and ρ_{hv} (0.90–0.95) values are characteristic of hail. As a result, this region is correctly classified as hail by HCA.

In brief, the conventional HDA (Witt et al. 1998) uses output from the storm cell identification and tracking (SCIT; Johnson et al. 1998) algorithm and Rapid Update Cycle (RUC)-estimates of the freezing level height to determine the probability of hail associated with each storm. Specifically, the probability of hail is linearly related to the height of the 45-dBZ echo above the freezing level. The resulting probability characterizes the associated SCIT-identified storm.

3. Data collection and verification methodology

During JPOLE, the S-band (11-cm) KOUN radar in Norman, Oklahoma, collected polarimetric data. According to the KOUN radar design, horizontally and vertically polarized radiation is transmitted and received simultaneously, which prohibits the measurement of linear depolarization ratio (LDR), a parameter frequently used for hail detection. Thus, it is important to determine how well hail may be detected without this variable.

Verification of observed polarimetric signatures was an important focus of JPOLE. During the course of the project (28 April–13 June 2003), two hail-intercept vehicles were used to intercept thunderstorm cores that had the potential to produce hail at the surface. The vehicles collected more than 28 hours of data on five separate days. These data included one isolated LP supercell storm on 1 May, one classic supercell storm on 19 May, two linearly aligned LP supercell storms on 11 June, and lines of convective storm cells on 14 May and 10 June, all within 150 km of KOUN.

The algorithms' (JPHCA, HCA, and HDA) respective products were tested against the ground truth dataset collected by the hail-intercept vehicles for several observations spanning four cases. These data included the isolated

LP supercell storm, the classic supercell storm, and lines of convective storm cells. JPHCA and HCA were run using data collected by the polarimetric KOUN radar, whereas HDA was run using data collected by KTLX, the nearest operational WSR-88D radar (20 km northeast of KOUN). For the two linearly aligned LP supercell storm, only KOUN data were available. Thus, analyses of these storms pertain to the JPHCA and HCA only.

Observations from the chase teams were compared with KOUN JPHCA and HCA output at low levels (0.5° elevation) to validate the algorithms' ability to discriminate between rain and hail. For HDA, probabilities of 60% or higher were considered indicative of hail falling at the ground. Ground truth data included in this validation met a set of temporal and spatial criteria. First, each hail report must occur within ± 6 min of available radar data (both KOUN and KTLX). Second, the observation must be located within an acceptable distance of either the 40-dBZ or higher reflectivity contour or a region of positive HCA hail classification. This distance, or radius of influence, varied from 3.2 to 5 km, depending on the speed of storm movement.

The application of these criteria resulted in the validation of JPHCA, HCA, and HDA output for 47 reports of either hail or rain from six different storms. Using these results, a 2x2 contingency table was created for each day, and for all days combined. The contingency table was then used to compute the following measures: probability of detection (POD), probability of false alarm (POFA), false alarm rate (FAR), critical success index (CSI), and Heidke skill score (HSS; see Appendix for definitions).

4. Statistical results

For the four cases in this study, both JPHCA and HCA outperform HDA in terms of overall accuracy and skill (Table 1). The most striking performance improvements for JPHCA, relative to HDA, are a 41% increase in HSS and a 41% decrease in POFD. This substantial increase in HSS means that JPHCA classifies hail more skillfully than HDA, with respect to a random classification. The substantial decrease in POFD means that JPHCA is less likely to attain a false alarm than HDA when hail is not observed. Other considerable performance improvements in JPHCA, relative to HDA, include a 26% increase in CSI and a 29% decrease in FAR. The decrease in FAR means that false alarms are less likely when hail is classified by JPHCA rather than HDA. Interestingly, the POD remains essentially the same (increases in HCA by only 2%). Hence, increases in JPHCA's HSS and CSI, compared to HDA, arise mostly from a decrease in false alarms, rather than an increase in correct detections or "hits".

Further analysis of these cases shows that the lack of improvement in JPHCA's POD results primarily from missed detections during an isolated LP supercell storm, located about 140 km west of KOUN. Analyses of linearly aligned LP supercell storms observed by KOUN only revealed the same result: JPHCA has trouble detecting hail observed at the ground from LP storms.

Figure 2 shows an example of polarimetric properties and JPHCA output from the 1 May 2003 isolated LP supercell at 00:16 UTC. The white plus sign in Fig. 2 indicates the location of 4.45 cm hail reported by one of the hail intercept vehicles. In Fig. 2, the reported hail is located in a region where reflectivity values (45−50 dBZ) are well below the reflectivity threshold of 55 dBZ conventionally employed for hail, but Z_{DR} and ρ_{hv} values are similar to those associated with hail (0.0−0.5 and 0.95−0.98, respectively). Because JPHCA is heavily weighted by Z, it misclassifies this region as heavy rain.

By modifying the JPHCA from a two-dimensional to a one-dimensional fuzzy logic approach, the hail signal found in Z_{DR} and ρ_{hv} values is weighted more strongly, resulting in hail detection within the vicinity of the ground truth (Fig. 3). By applying the new HCA to the linearly aligned LP supercell storms observed by KOUN only, we find that all previously missed hail detections are correctly classified.

From a statistical standpoint, the "tuned" HCA eliminates former missed detections (POD = 100%) and thereby improves further the CSI (0.82 vs 0.89, respectively) and HSS (0.72 and 0.80, respectively), compared to JPHCA and HDA (Table 1). However, these improvements come with a slight cost, where POFD increases from 17% (JPHCA) to 25% (HCA). Note, however, that FAR remains the same (Table 1). Thus, improved detection of hail in LP supercell storms results in a slight increase in false detections when hail is not observed at the ground.

Table 1. JPOLE hydrometeor classification algorithm (JPHCA), tuned HCA, and legacy WSR-88D hail detection algorithm (HDA) accuracy and skill measures, given as percentages, excluding CSI, and HSS, which range from 0 to 1. Probabilities are rounded to the nearest integer.

Algorithm	POD	POFD	FAR	CSI	HSS
JPHCA	90	17	10	0.82	0.72
HCA	100	25	11	0.89	0.80
HDA	88	58	39	0.56	0.31

5. Summary and conclusions

This study illustrates the applicability of polarimetric data for hail detection. A statistical comparison of performance measures for the JPOLE HCA (JPHCA) and conventional HDA shows substantial improvement in the critical success index (CSI; 24%), Heidke skill score (HSS; 41%), probability of false alarm (POFA; 41%), and false alarm rate (FAR; 29%). The primary shortcoming of JPHCA is missed hail detections during LP supercell storms. Modifying the JPHCA from a two-dimensional- to a one-dimensional-fuzzy logic algorithm solves this problem. As a result, the probability of detection (POD) increases from 90 to 100%, CSI increases from 0.82 to 0.89, FAR remains approximately the same, and POFA increases from 17 to 25%.

The superior performance of JPHCA and HCA, compared to HDA, demonstrates the advantage of using polarimetric variables Z_{DR} and ρ_{hv}, in addition to Z, to discriminate between hail and rain. These results indicate that
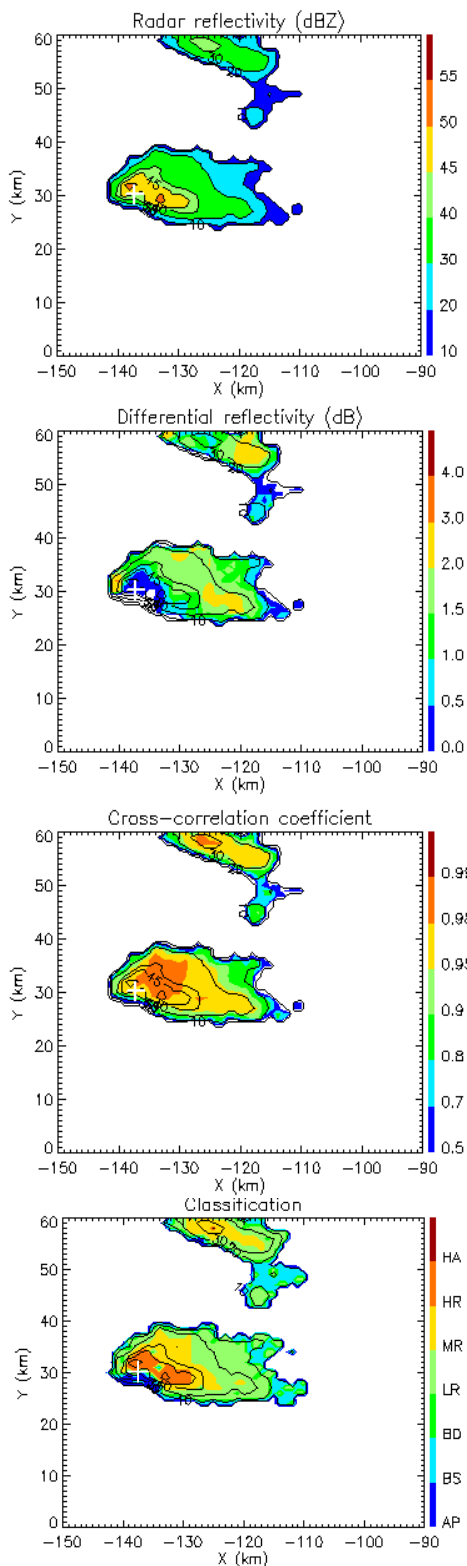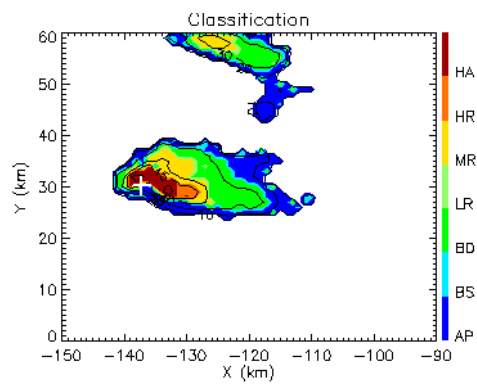
Fig. 3. Tuned hydrometeor classification fields at the same date and time as the LP supercell storm shown in Fig. 2. The white cross denotes the location of a 4.45-cm hailstone.

high performance can be achieved without using LDR. These positive results, coupled with HCA's ability to pinpoint the location of hail within a storm, show that the polarimetric WSR-88D radar promises significant improvement in detection of hail.

References

Aydin, K., T. A. Seliga, and V. Balaji, 1986: Remote sensing of hail with a dual linear polarization radar. *J. Appl. Meteor.,* **25,** 1475–1484.

Balakrishnan, N., and D. S. Zrnić, 1990: Use of polarization to characterize precipitation and discriminate large hail. *J. Atmos. Sci.,* **47,** 1525–1540.

Bringi, V. N., and V. Chandrasekar, 2001: *Polarimetric Doppler Weather Radar: Principles and Applications.* Cambridge University Press, 636 pp.

Hubbert, J., V. N. Bringi, L. D. Carey, and S. Bolen, 1998: CSU–CHILL polarimetric radar measurements from a severe hail storm in eastern

Fig. 2. Fields of (a) reflectivity, (b) differential reflectivity, (c) JPOLE hydrometeor classification and (d) cross-correlation coefficient for a low-precipitation (LP) supercell storm at 00:16 UTC on 1 May 2003. The white cross denotes the location of a 4.45-cm hailstone.

Colorado. *J. Appl. Meteor.*, **37,** 749–775.

Johnson, J. T., P. L. MacKeen, A. Witt, E. D. Mitchell, G. J. Stumpf, M. D. Eilts, and K. W. Thomas, 1998: The storm cell identification and tracking algorithm: An enhanced WSR–88D algorithm. *Wea. Forecasting,* **13,** 263–276.

Kennedy, P. C., S. A. Rutledge, W. A. Peterson, and V. N. Bringi, 2001: Polarimetric radar observations of hail formation. *J. Appl. Meteor.,* **40**, 1347–1366.

Liu, H., and V. Chandrasekar, 2000: Classification of hydrometeors based on polarimetric radar measurements: Development of fuzzy logic and neuro-fuzzy systems, and in situ verification. *J. Atmos. Oceanic Technol.*, **17,** 140–164.

Ryzhkov, A. V., S. Giangrande, and T. Schuur, 2003: Rainfall measurements with the polarimetric WSR–88D radar. Report of the National Severe Storms Laboratory, 98 pp. [Available from NOAA/National Severe Storms Laboratory, 1313 Halley Circle, Norman, OK 73069.].

Schuur, T., A. Ryzhkov, P. Heinselman, D. Zrnić, D. Burgess, and K. Scharfenberg, 2003: Observation and classification of echoes with polarimetric WSR–88D radar. Report of the National Severe Storms Laboratory, 46 pp. [Available from NOAA/National Severe Storms Laboratory, 1313 Halley Circle, Norman, OK 73069.].

Smith, P. L., D. J. Musil, A. G. Detwiler, and R. Ramachandran, 1999: Observations of mixed-phase precipitation within a CaPE thunderstorm. *J. Appl. Meteor*., **38**, 145–155.

Straka, J. M., D. S. Zrnić, and A. V. Ryzhkov, 2000: Bulk hydrometeor classification and quantification using polarimetric radar data: A synthesis of relations. *J. Appl. Meteor.,* **39,** 1341–1372.

Vivekanandan, J., D. Zrnić, S. Ellis, D. Oye, A. Ryzhkov, and J. Straka, 1999: Cloud microphysics retrieval using S-band dual-polarization radar measurements. *Bull. Amer. Meteor. Soc.*, **80,** 381–388.

Witt, A., M. D. Eilts, G. J. Stumpf, J. T. Johnson, E. D. Mitchell, and K.W. Thomas, 1998: An enhanced hail detection algorithm for the WSR–88D. *Wea. Forecasting,* **13**, 286–303.

Zrnić, D. S., and A.V. Ryzhkov, 1999: Polarimetry for weather surveillance radars. *Bull. Amer. Meteor. Soc.*, **80**, 389–406.

_____, _____, J. Straka, Y. Liu, and J. Vivekanandan, 2001: Testing a procedure for the automatic classification of hydrometeor types. *J. Atmos. Oceanic Technol.*, **18,** 892–913.

Appendix: Accuracy and Skill Scores

The 2x2 contingency tables were constructed by comparing algorithm detections to ground truth, where *a* is a "hit", *b* is a "false alarm", *c* is a "miss", and *d* is a "correct null". For each case, and all cases combined, we examined three accuracy measures, including probability of detection (POD), where

$$\text{POD} = \frac{a}{a+c} \qquad (1A),$$

probability of false detection (POFD), where

$$\text{POFD} = \frac{b}{b+d} \qquad (2A),$$

$$\text{FAR} = \frac{b}{a+b} \qquad (3A),$$

and critical success index (CSI), where

$$\text{CSI} = \frac{a}{a+b+c} \qquad (4A).$$

Each of these measures ranges from 0 to 1, though POD and POFD are typically expressed in terms of

percentages. A perfect forecast would have a POD of 100%, a POFD of 0%, and a CSI of 1. Additionally, we examined the Heidke skill score (HSS),

$$\text{HSS} = \frac{2(ad - bc)}{(a+c)(c+d)+(a+b)(b+d)} \quad (5A),$$

to assess the skill of the algorithms compared to a random forecast. The HSS ranges from 0 to 1, with a perfectly skillful forecast having a value of 1.